ORIGINAL ARTICLE

GET4 is a novel driver gene in colorectal cancer that regulates the localization of BAG6, a nucleocytoplasmic shuttling protein

Kensuke Koike[1,2] | Takaaki Masuda[1] | Kuniaki Sato[3] | Atsushi Fujii[1] |
Hiroaki Wakiyama[1] | Taro Tobo[4] | Junichi Takahashi[1] | Yushi Motomura[1] |
Takafumi Nakano[1] | Hideyuki Saito[1] | Yoshihiro Matsumoto[1] | Hajime Otsu[1] |
Kazuki Takeishi[1] | Yusuke Yonemura[1] | Koshi Mimori[1] | Takashi Nakagawa[3]

[1]Department of Surgery, Kyushu University Beppu Hospital, Beppu, Japan

[2]Department of Otorhinolaryngology, Graduate School of Medical Sciences, Kyushu University, Fukuoka, Japan

[3]Department of Head and Neck Surgery, National Hospital Organization Kyushu Cancer Center, Fukuoka, Japan

[4]Department of Pathology, Kyushu University Beppu Hospital, Beppu, Japan

Correspondence
Koshi Mimori, Department of Surgery, Kyushu University Beppu Hospital, 4546 Tsurumihara, Beppu 874-0838, Japan.
Email: kmimori@beppu.kyushu-u.ac.jp

Funding information
Japan Society for the Promotion of Science (JSPS) Grant-in-Aid for Science Research, Grant/Award Number: 18K08649, 19K09176, 19H03715, 20H05039 and 20K08930; OITA Cancer Research Foundation; AMED, Grant/Award Number: JP20cm0106475h0001; Takeda Science Foundation

Abstract

Colorectal cancer (CRC) is one of the most common types of cancer and a significant cause of cancer mortality worldwide. Further improvements of CRC therapeutic approaches are needed. BCL2-associated athanogene 6 (BAG6), a multifunctional scaffold protein, plays an important role in tumor progression. However, regulation of BAG6 in malignancies remains unclear. This study showed that guided entry of tail-anchored proteins factor 4 (GET4), a component of the BAG6 complex, regulates the intercellular localization of BAG6 in CRC. Furthermore, GET4 was identified as a candidate driver gene on the short arm of chromosome 7, which is often amplified in CRC, by our bioinformatics approach using the CRC dataset from The Cancer Genome Atlas. Clinicopathologic and prognostic analyses using CRC datasets showed that GET4 was overexpressed in tumor cells due to an increased DNA copy number. High GET4 expression was an independent poor prognostic factor in CRC, whereas BAG6 was mainly overexpressed in the cytoplasm of tumor cells without gene alteration. The biological significance of GET4 was examined using GET4 KO CRC cells generated with CRISPR-Cas9 technology or transfected CRC cells. In vitro and in vivo analyses showed that GET4 promoted tumor growth. It appears to facilitate cell cycle progression by cytoplasmic enrichment of BAG6-mediated p53 acetylation followed by reduced p21 expression. In conclusion, we showed that GET4 is a novel driver gene and a prognostic biomarker that promotes CRC progression by inducing the cytoplasmic transport of BAG6. GET4 could be a promising therapeutic molecular target in CRC.

KEYWORDS
BAG6, cell cycle, colorectal cancer, driver gene, GET4

1 | INTRODUCTION

Colorectal cancer (CRC) is one of the most commonly diagnosed cancers and among the leading causes of cancer death worldwide, and improved strategies for CRC treatment are needed.[1-3] Identification of new therapeutic molecular targets in CRC cells is required.

The unique multidomain protein BCL2-associated athanogene 6 (BAG6) is a multifunctional scaffold protein.[4] It contributes to a diverse range of cellular processes, such as protein quality control and membrane protein translocation, by interacting with its target proteins for shuttling to distinct destinations.[4-8] Moreover, BAG6 modulates apoptosis, gene regulation, histone acetylation, and autophagy in a manner dependent on its nucleocytoplasmic localization.[4,9-13] Of note, it has been shown that nuclear export of BAG6 inhibits cancer cell apoptosis in CRC.[14] These reports suggest that BAG6 could play an important role in tumor progression. However, the regulation of BAG6 has been unclear in malignancies, including CRC.

Detailed studies reported that BAG6 forms a complex with its cytoplasmic retention factor, guided entry of tail-anchored proteins factor 4 (GET4).[9] Masking of its nuclear localization signal (NLS) by GET4 leads to preferential cytosolic localization of BAG6.[4,9,15,16] The genes comprising the BAG6 complex could include driver genes that control the localization of BAG6 and consequent CRC progression.

Chromosomal amplification is considered a strong driving force during cancer progression.[17] We reported that the amplification of chromosomes, including chromosome 7 (Ch.7), is a fundamental and predominant event in CRC development.[18,19] These observations suggest that Ch.7 harbors driver genes that are overexpressed due to chromosomal amplification.[20] In fact, we recently identified several novel driver genes in CRC such as eIF5-mimic protein 1, CRMP5-associated GTPase, phosphoserine phosphatase, and DEAD-box helicase 56 on the short arm of chromosome 7 (Ch.7p).[21-24] Interestingly, *GET4* is located on Ch.7p.

In this study, we identified *GET4* as a novel driver gene that promotes tumor growth, possibly by controlling the subcellular localization of BAG6 in CRC. This finding suggests opportunities for developing molecular therapeutic target therapy.

2 | MATERIALS AND METHODS

2.1 | Public datasets

The Cancer Genome Atlas database (TCGA), accessed through the Broad Institute's Firehose site (http://gdac.broadinstitute.org), was analyzed in this study, and we obtained mRNA expression data of 17 CRC patients from the GSE32323 dataset through the GEO database (http://www.ncbi.nlm.nih.gov). We also obtained normalized mRNA expression data and DNA copy number data from 60 available CRC cell lines from the CCLE dataset (http://www.broadinstitute.org/ccle/home). A TCGA cohort from the LinkedOmics database (http://www.linkedomics.org/login.php) was used to evaluate the correlation between subject genes and the overall survival (OS)

of patients. The subject gene alterations with mutations were detected in the Catalogue of Somatic Mutations in Cancer (COSMIC) dataset (https://cancer.sanger.ac.uk/cosmic).

The mRNA expression datasets from TCGA for pan-cancer expression analysis were obtained from liver hepatocellular carcinoma (LIHC; 371 tumor tissues, 50 noncancerous tissues), bladder urothelial carcinoma (BLCA; 407 tumor tissues, 19 noncancerous tissues), cholangiocarcinoma (CHOL; 36 tumor tissues, 9 noncancerous tissues), colorectal adenocarcinoma (COADREAD; 380 tumor tissues, 51 noncancerous tissues), esophageal carcinoma (ESCA; 184 tumor tissues, 11 noncancerous tissues), pancreatic adenocarcinoma (PAAD; 178 tumor tissues, 4 noncancerous tissues), lung adenocarcinoma (LUAD; 515 tumor tissues, 59 noncancerous tissues), lung squamous cell carcinoma (LUSC; 502 tumor tissues, 51 noncancerous tissues), stomach adenocarcinoma (STAD; 415 tumor tissues, 35 noncancerous tissues), glioblastoma (GBM; 154 tumor tissues, 5 noncancerous tissues), head and neck squamous cell carcinoma (HNSC; 520 tumor tissues, 44 noncancerous tissues), prostate adenocarcinoma (PRAD; 497 tumor tissues, 52 noncancerous tissues), breast invasive carcinoma (BRCA; 1097 tumor tissues, 114 noncancerous tissues), kidney renal clear cell carcinoma (KIRC; 533 tumor tissues, 72 noncancerous tissues), and uterine corpus endometrial carcinoma (UCEC; 176 tumor tissues, 24 noncancerous tissues). The TCGA data were normalized by quantile normalization.[25]

2.2 | Selection of candidate driver genes with TCGA dataset

We used RNA sequencing data of 623 CRC patients, DNA copy number data of 615 CRC patients, and clinical data in TCGA from the Broad Institute's Firehose (http://gdac.broadinstitute.org/runs/stddata__2016_01_28/data/COADREAD/20160128). The RNA sequencing data also included the expression profiles of 51 paired normal colon samples. As Figure S1 shows, by using these data, we extracted candidate driver genes from 426 genes on Ch.7p that showed positive correlations between the DNA copy number and mRNA expression levels (threshold of the correlation coefficient, 0.4) as criteria 1 and was significantly overexpressed in tumor tissues compared with normal tissues (>1.5-fold change) as criteria 2.

2.3 | Human CRC cell lines

In this study, we used various cancer cell lines including CRC (colo205, colo320, SW480, and SW620), gastric cancer (MKN45), esophageal squamous cell carcinoma (TE6), lung adenocarcinoma (H1650), hepatocellular carcinoma (HepG2 and PLC), and cholangiocarcinoma (RBE). Six cell lines (SW620, COLO205, COLO320, TE6, HepG2, and RBE), SW480, MKN45, H1650, and PLC were purchased from RIKEN BioResource Center, ATCC, Japanese Collection of Research Bioresources Cell Bank, The University of Tokyo Graduate School of Frontier Sciences, and KAC, respectively. Seven cell lines (SW620,

SW480, COLO205, MKN45, TE6, H1650, and RBE) and three cell lines (COLO320, HepG2, and PLC) cells were cultured in RPMI-1640 and DMEM, respectively. All media were supplemented with 10% FBS with 100 U/mL penicillin and 100 U/mL streptomycin sulfate. All cells were maintained in a humidified atmosphere containing 5% CO_2 at 37°C.

2.4 | Total RNA extraction and RT-quantitative PCR

Total RNA from cell lines was extracted using ISOGEN-II (Nippon Gene). Reverse transcription was carried out using 8 μg total RNA with M-MLV reverse transcriptase (Nippon Gene), according to the manufacturer's instructions. Quantitative PCR (qPCR) was undertaken using LightCycler FastStart DNA Master SYBR Green I (Roche Diagnostics) as previously described.[26] The expression levels of GET4 and p21 mRNA were normalized to 18S mRNA as an internal control, and they were expressed as values relative to the expression level of the cDNA from Human Universal Reference Total RNA (Clontech). The primer sequences for qPCR were as follows: GET4, forward 5′-AGAAGGGCGACTACTACGAGG-3′ and reverse 5′-GGGCTCCCGAGTACATGAGC-3′; p21, forward 5′-GCGAC TGTGATGCGCTAATG-3′ and reverse 5′-GAAGGTAGAGCTTGGG CAGG-3′; and 18S, forward 5′-AGTCCCTGCCCTTTGTACACA-3′ and reverse 5′-CGATCCGAGGGCCTCACTA-3′.

2.5 | Immunohistochemical analysis

Immunohistochemical analysis of CRC tissue samples and tissue specimens from mouse xenograft tumors was carried out as previously described.[27] All sections were counterstained with hematoxylin. The primary Abs used were as follows: anti-GET4 Ab (1:500; Atlas Antibodies), anti-BAG6 Ab (1:200; Atlas Antibodies), and anti-Ki67 Ab (1:10 000; Abcam). Tumor histology was independently carried out by an experienced research pathologist at Kyushu University Beppu Hospital.

2.6 | Protein extraction and immunoblotting analysis

For total protein extraction, cells were lysed in lysis buffer (25 mM Tris-HCl [pH 7.5], 0.2 mM EDTA, 150 mM NaCl, 0.1% NP40, 5% glycerol, and proteinase inhibitor cocktail). Immunoblotting analysis was carried out as previously described.[28] Briefly, equal amounts of protein (30 μg) were electrophoresed on 4%-20% or 10% Tris-glycine polyacrylamide gels and then transferred to Immobilon-P Transfer Membranes (Merck Millipore) at 70 V for 4 hours at room temperature or 30 V overnight at 4°C. Nonspecific binding sites were blocked with blocking buffer (TBS and 0.1% Tween-20 with 5% nonfat milk powder) for 1 hour at room temperature, and the blot was incubated at 4°C overnight

with the following specific primary Abs in blocking buffer (anti-GET4 at 1:250 dilution; anti-p21, anti-p53, and anti-β-actin at 1:1000 dilution; anti-p53 [acetyl K373] at 1:5000 dilution). After washing, the blots were incubated with an appropriate secondary Ab conjugated with HRP for 1 h at room temperature. The blots were washed again and the detection was undertaken using FUSION SOLO S (VILBER). Rabbit polyclonal Abs targeting GET4 were purchased (Atlas Antibodies). Rabbit polyclonal Abs targeting p21 were purchased (Cell Signaling Technology). Mouse mAbs targeting β-actin were purchased (Santa Cruz Biotechnology). Rabbit polyclonal Abs targeting p53 (acetyl K373) and mouse mAbs targeting p53 were purchased (Abcam). Protein concentrations were quantified using the BCA Protein Assay Kit (Thermo Fisher Scientific).

2.7 | Immunofluorescence analysis

Cells were plated on Lab-Tek Chamber Slides (Thermo Fisher Scientific) and incubated at 37°C under 5% CO_2 overnight. Before staining the cells, they were washed with PBS and fixed in a methanol solution. After the cells were washed with PBS, they were incubated in 1% BSA in PBS for 1 h at room temperature. After the anti-BAG6 Ab (Atlas Antibodies; 1:200) had been used as the primary Ab, the cells were incubated at 4°C overnight. The next day, they were washed with PBS and incubated with AlexaFluor 488 (Cell Signaling Technology; 1:1000) as the secondary Ab for 1.5 hours at room temperature. After washes with PBS, the cells were stained with SlowFade Diamond Antifade Mountant with DAPI (Thermo Fisher Scientific). Images were acquired by using fluorescence microscopy (BZ-X700; Keyence). We then counted the number of cells stained by Ab against BAG6.

2.8 | GET4 siRNA transfection

GET4-specific siRNAs (Silencer Predesigned siRNA #1, sense CGGUGG UCUUCACGACGUATT and antisense UACGUCGUGAAGACCACCGAT; Silencer Predesigned siRNA #2, sense AGAUGUACCGGACCCUGUUTT and antisense AACAGGGUCCGGUACAUCUGG) and negative control siRNA (Silencer Negative Control 1 siRNA) were purchased (Ambion). According to the manufacturer's instructions, transfection of SW620 or SW480 cells with siRNA oligonucleotides was undertaken using Lipofectamine RNAiMAX (Thermo Fisher Scientific).

2.9 | Generation of GET4 KO CRC cells and rescue studies of GET4 by GET4 transient transfection

The GET4 KO SW620 cells and SW480 cells were generated using the All-in-One CRISPR-Cas9[D10A] nickase-based system as previously described.[29] First, specific guide RNAs targeting different regions of the GET4 gene were designed by a free online survey

tool: CRISPRdirect (http://crispr.dbcls.jp) and cloned into the All-in-One CRISPR-Cas9 vector (Addgene). The transfection of the GFP-labeled Cas9 nickase was carried out using Lipofectamine 3000 (Thermo Fisher Scientific) according to the manufacturer's instructions for 48 hours, and GFP-positive cells were sorted by an SH800 cell sorter (Sony Biotechnology). To obtain different monoclonal cell populations, single-cell cloning was carried out. Verification of appropriate targeted DNA clones was undertaking by genotyping PCR. Primers used for genotyping PCR were as follows: forward 5′-TGTATAGCTCAATGGCTGCTGT-3′ and reverse 5′-ACTTCCAAGCGGTCACAGTC-3′. Furthermore, the cells were confirmed as GET4 KO clones by immunoblotting analysis and sanger sequencing. Rescue studies were carried out using pLenti-GIII-CMV-*GET4* vector (Applied Biological Materials). As a negative control, we used p3xFLAG-CMV-9 and 10 Expression Vector (Sigma-Aldrich). We transfected the vectors for GET4 KO SW620 cells and SW480 cells using Lipofectamine 3000 (Thermo Fisher Scientific) following the manufacturer's protocol.

2.10 | Colony formation assay

Changes in the proliferation of SW620 and SW480 cells by GET4 knockdown or KO were examined using colony formation assays. For GET4 KO studies, cells were plated at a density of 1000 cells/well (SW620) or 3000 cells/well (SW480) in triplicate in 6-well plates and incubated in a humidified atmosphere containing 5% CO_2 at 37°C. For siRNA-mediated GET4 knockdown studies, cells were plated at a density of 3000 cells/well in 6-well plates and incubated at 37°C under 5% CO_2 overnight. Cells were then transfected with *siGET4* or negative control siRNA in triplicate using Lipofectamine RNAiMAX (Thermo Fisher Scientific). For GET4 rescue studies, GET4 KO SW620 and SW480 cells were plated at a density of 3000 cells/well in 6-well plates and incubated at 37°C under 5% CO_2 overnight. Cells were transiently transfected with a vector expressing GET4 to rescue GET4 or a control vector in triplicate using Lipofectamine 3000 (Thermo Fisher Scientific). After 14 days, the colonies were stained using a Differential Quick Strain Kit (Sysmex) according to the manufacturer's instructions. For appropriate counts, visible colonies were photographed using a FUSION SOLO S (VILBER). Colony counts were determined using ImageJ software (version 1.80; NIH).

2.11 | Murine xenograft model

All animal procedures were undertaken in compliance with the Guidelines for the Care and Use of Experimental Animals established by the Committee for Animal Experimentation of Kyushu University. Murine xenograft model analysis was carried out as previously described.[21] Five-week-old female BALB/c nu/nu mice were purchased from Japan SLC and kept under specific pathogen-free conditions. For subcutaneous xenograft assays, 1×10^6 WT cells or GET4 KO SW620 cells were suspended in 100 μL of 50% Matrigel (Corning) in PBS and injected bilaterally into nude mice. Tumor sizes were calculated using the following formula: length × width^2 × 0.5.

2.12 | Cell cycle assay

Cells were synchronized at the G_1 phase of the cell cycle by serum starvation for 96 hours and restimulated by changing medium containing 10% FBS as previously described.[21] The restimulated cells were harvested, washed with PBS, and fixed in 70% ethanol at −20°C. The fixed cells were incubated in 0.25 mg/mL RNase for 30 minutes at 37°C. Samples were then washed with PBS and stained with propidium iodide (Sigma-Aldrich). The cell cycle distribution was measured on an SH800 cell sorter (Sony Biotechnology).

An EdU assay was carried out using GET4 KO cells and WT cells in the medium containing 10% FBS. Cells were incubated with EdU for 2 hours before harvest. EdU was detected using a Click-iT Plus EdU Alexa Fluor 488 Flow Cytometry Assay Kit (Thermo Fisher Scientific) following the manufacturer's instructions. The cell cycle distribution was measured on an SH800 cell sorter (Sony Biotechnology).
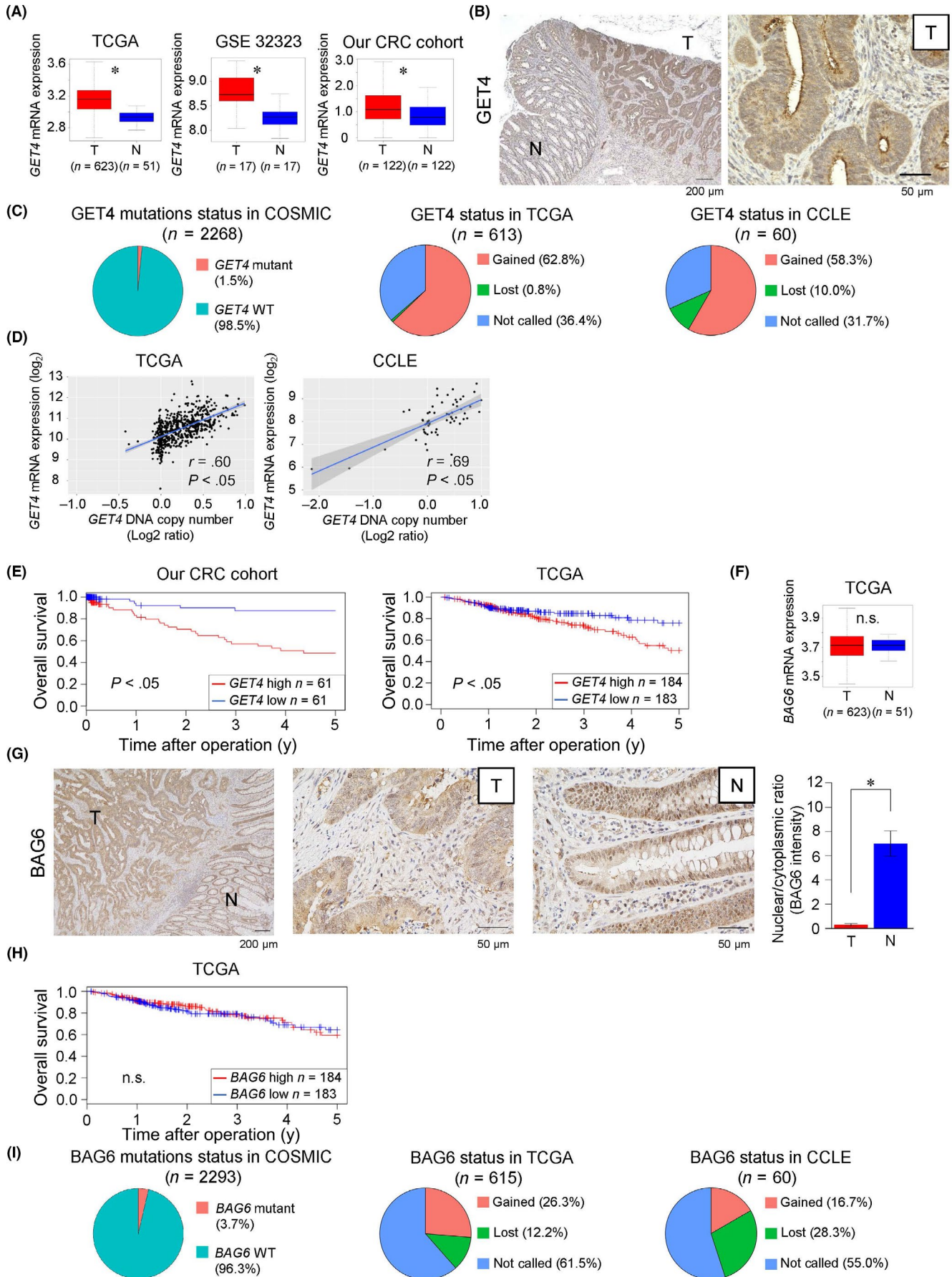
2.13 | Patients with CRC and collection of clinical samples

A total of 122 patients with CRC who underwent surgical resection of a primary tumor at Kyushu University Beppu Hospital and its affiliated hospitals between 1992 and 2007 were enrolled in this study. Sample collection was carried out as previously described.[28] All patients were treated following the Japanese Society of Cancer of the Colon and Rectum Guidelines for the Treatment of Colorectal Cancer. Written informed consent was obtained from all patients, and the Institutional Review Board of Kyushu University approved this study (approval no. 2020-302).

2.14 | Statistical analysis

Associations between variables were analyzed using Student's *t* test, the Mann-Whitney *U* test, or Fisher's exact test. The degree of linearity was assessed by Pearson's correlation coefficient. Overall survival was estimated using the Kaplan-Meier method, and survival curves were compared using the log-rank test. Data analyses were undertaken using JMP Pro version 15 software (SAS Institute) and R software version 4.0.3 (The R Foundation). Two-sided $P < .05$ was deemed statistically significant (*$P < .05$).

(A) TCGA, GSE 32323, Our CRC cohort — GET4 mRNA expression

(B) GET4 immunohistochemistry

(C) GET4 mutations status in COSMIC (n = 2268); GET4 status in TCGA (n = 613); GET4 status in CCLE (n = 60)

(D) TCGA (r = .60, P < .05); CCLE (r = .69, P < .05)

(E) Our CRC cohort (P < .05); TCGA (P < .05)

(F) TCGA — BAG6 mRNA expression

(G) BAG6 immunohistochemistry; Nuclear/cytoplasmic ratio (BAG6 intensity)

(H) TCGA — Overall survival

(I) BAG6 mutations status in COSMIC (n = 2293); BAG6 status in TCGA (n = 615); BAG6 status in CCLE (n = 60)

FIGURE 1 Identification of candidate driver genes on chromosome 7p in colorectal cancer (CRC). A, Left, *GET4* mRNA expression in 623 CRC tissues and 51 normal colon tissues obtained from The Cancer Genome Atlas (TCGA) dataset. Middle, *GET4* mRNA expression in 17 CRC tissues and paired normal colon tissues in the GSE 32323 dataset. Right, *GET4* mRNA expression assessed by RT-quantitative PCR in 122 CRC tissues and paired normal colon tissues in our dataset. *$P < .05$. B, Immunohistochemical staining for GET4. Scale bar, 200 μm (left) and 50 μm (right). N, normal tissue; T, tumor tissue. C, Left, The frequency of mutations was 1.5% in GET4 among CRC cases in the COSMIC dataset. Middle, Status of GET4 in 613 CRC tissues in TCGA dataset. Right, Status of GET4 in 60 CRC tissues in the CCLE dataset. Gained, $\log_2$ copy number ratios >0.1; Lost, $\log_2$ copy number ratios <−0.1; Not called, −0.1 < $\log_2$ copy number ratios < 0.1. D, Left, Correlation between GET4 copy number and *GET4* mRNA expression in the TCGA dataset. Right, Correlation between GET4 copy number and *GET4* mRNA expression in the CCLE dataset. *r*, Pearson's correlation coefficient. E, Left, Overall survival rate in CRC patients according to *GET4* mRNA expression in tumor tissues in our dataset. Right, Overall survival rate in CRC patients according to *GET4* mRNA expression in tumor tissues in the TCGA cohort using the LinkedOmics database. F, *BAG6* mRNA expression between 623 CRC tissues (T) and 51 normal colon tissues (N) in the TCGA dataset. n.s., not significant. G, Immunohistochemical staining for BAG6 in the normal colon (N) or tumor tissues (T). Scale bar, 200 μm (left) and 50 μm (middle and right). The bar graph shows the nuclear / cytoplasmic ratio of BAG6 intensity in the normal colon or tumor tissues. More than 200 cells were counted in each. *$P < .05$. H, Overall survival rate in CRC patients according to *BAG6* mRNA expression in tumor tissues in the TCGA cohort using the LinkedOmics database. n.s., not significant. I, Left, The frequency of mutations was 3.7% in BAG6 among CRC cases in the COSMIC dataset. [Correction added on 18 December 2021, after first online publication: In Figure 1I caption, the dataset 'TCGA' in Left was corrected to 'COSMIC' in this version.] Middle, Status of BAG6 in 615 CRC tissues in the TCGA dataset. Right, Status of BAG6 in 60 CRC tissues in the CCLE dataset. Gained, $\log_2$ copy number ratios >0.1; Lost, $\log_2$ copy number ratios <−0.1; Not called, −0.1 < $\log_2$ copy number ratios < 0.1

TABLE 1 Univariate and multivariate analyses of clinicopathologic factors affecting overall survival in study patients with colorectal cancer

Factors	Univariate analysis			Multivariate analysis		
	HR	95% CI	*P* value	HR	95% CI	*P* value
Age (≥65/<65)	0.74	0.38-1.48	.40	–	–	–
Gender (male/female)	1.19	0.61-2.35	.61	–	–	–
Histology (poorly/well, moderately)	4.48	1.72-11.70	<.05	3.93	1.40-11.04	<.05
Depth of invasion (SS/SE/SI / M/SM/MP)	6.32	1.51-26.40	<.05	2.02	0.43-9.41	.37
Lymphatic invasion (present/absent)	3.90	1.89-8.03	<.05	3.03	1.39-6.59	<.05
Lymph node metastasis (present/absent)	7.26	2.80-18.80	<.05	3.51	1.24-9.94	<.05
Vascular invasion (present/absent)	1.63	0.83-3.21	.16	–	–	–
GET4 mRNA expression (high/low)	4.85	2.01-11.70	<.05	5.21	2.11-12.84	<.05

Abbreviations: –, not included in analysis; CI, confidence interval; HR, hazard ratio; M, mucosa; MP, muscular propria; SE, serosal invasion; SI, invasion to adjacent organs; SM, submucosa; SS, subserosa.

3 | RESULTS

3.1 | *GET4* is a potential driver gene in CRC

We identified 21 candidate driver genes that satisfied the criteria that we established (Figure S1A). Among these genes, we focused on *GET4* because this gene regulates the localization of BAG6, which could be associated with CRC progression depending on its localization.[9,14]
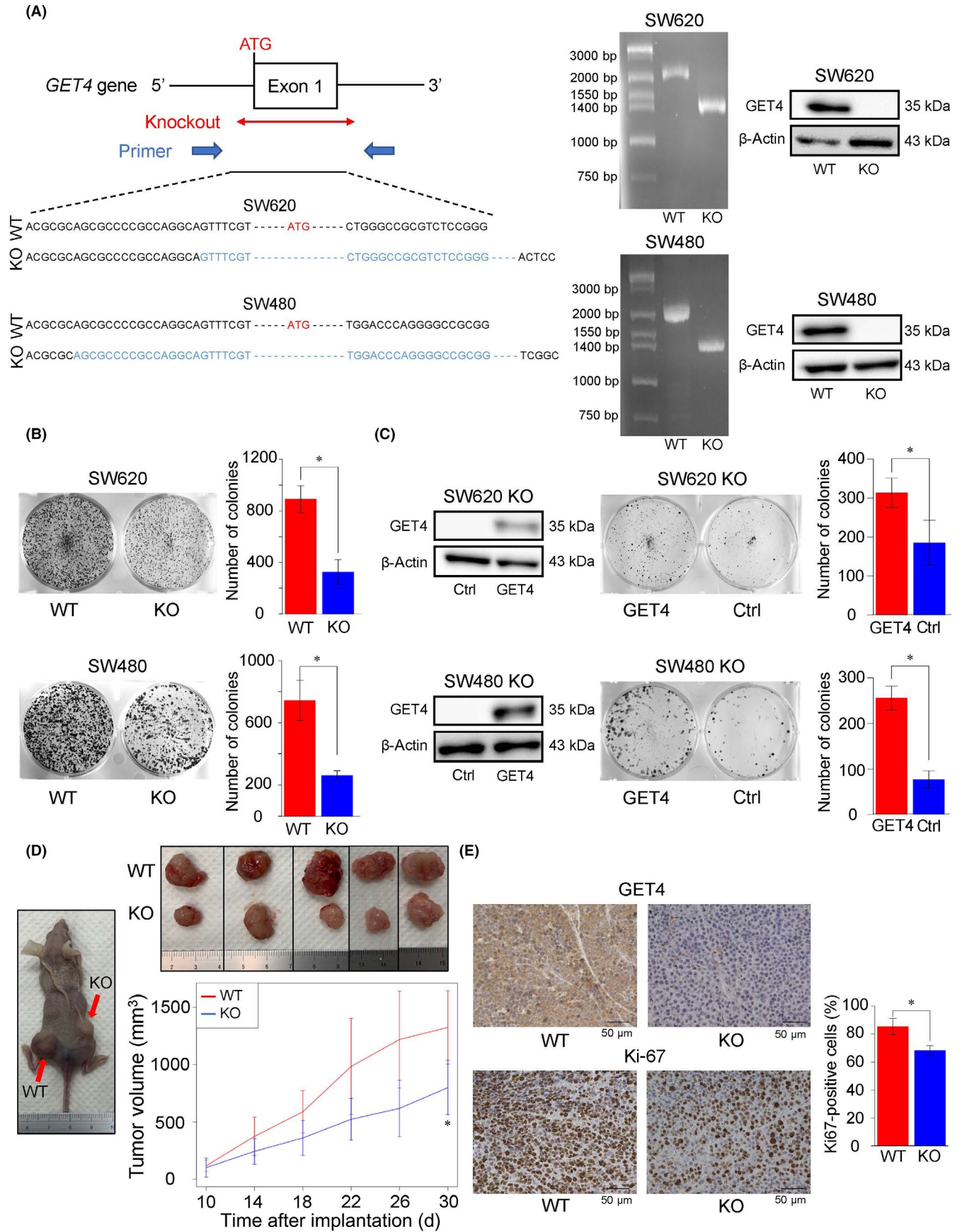
GET4 mRNA expression in tumor tissues was higher than in normal tissues (Figure 1A). In immunohistochemical analysis, GET4 stained more intensely in the nuclei and cytoplasm of CRC tumor cells than normal colon cells (Figure 1B). In genomic analysis, only 1.5% of *GET4* gene alterations with mutations were detected in the COSMIC dataset (Figure 1C). Moreover, amplification of *GET4* was observed in 62.8% of 613 CRC samples in the TCGA dataset, and in 58.3% of 60 CRC samples in the CCLE dataset ($\log_2$ copy number ratios >0.1) (Figure 1C). *GET4* mRNA expression and copy numbers were positively correlated in the TCGA dataset and the CCLE dataset (Figure 1D).

These results provide evidence that GET4 is overexpressed in tumor cells due to increased DNA copy numbers in CRC, suggesting that *GET4* could be a candidate driver gene in CRC.

3.2 | High expression of *GET4* mRNA in tumor tissues predicts a poor prognosis in CRC patients

We evaluated subjects' survival rates according to *GET4* mRNA expression in CRC. We used the LinkedOmics database and divided the patients into two groups at the median value of *GET4* mRNA expression. In our hospital dataset and TCGA cohort, the patients with high *GET4* mRNA expression had significantly lower OS than patients with low expression (Figure 1E). In the univariate analysis, poor histology, higher T factor (≥subserosa), lymphatic invasion, lymph node metastasis, and high *GET4* mRNA expression were

(A)

GET4 gene 5' —[Exon 1]— 3'
ATG

Knockout

Primer

SW620

SW620
WT: ACGCGCAGCGCCCCGCCAGGCAGTTTCGT-----ATG----CTGGGCCGCGTCTCCGGG
KO: ACGCGCAGCGCCCCGCCAGGCAGTTTCGT-------------CTGGGCCGCGTCTCCGGG-----ACTCC

SW480
WT: ACGCGCAGCGCCCCGCCAGGCAGTTTCGT-----ATG----TGGACCCAGGGGCCGCGG
KO: ACGCGCAGCGCCCCGCCAGGCAGTTTCGT-------------TGGACCCAGGGGCCGCGG-----TCGGC

(B) SW620, SW480 colony assays

(C) SW620 KO, SW480 KO

(D) Tumor volume (mm³) vs Time after implantation (d)

(E) GET4, Ki-67; Ki67-positive cells (%)

FIGURE 2 Effects of GET4 KO on cell proliferation in colorectal cancer (CRC) cells. A, Left, Direct sequencing analysis confirmed successful genome editing of *GET4* exon 1. Middle, RT-PCR of gene-targeted *GET4*. WT, 2100 bp; KO, approximately 1300 bp. Right, Immunoblotting for GET4 in WT cells and GET4 KO cells. B, Colony formation assays using GET4 KO SW620 and SW480 cells. C, Left, GET4 protein levels in the indicated cells. Immunoblotting for GET4 in these rescued cells. Right, Colony formation assays using indicated cells. D, In vivo analysis using xenograft mouse models. Tumor size using WT cells or GET4 KO CRC cells. E, Immunohistochemical staining for GET4 or Ki-67 in tumor tissues from WT cells and GET4 KO CRC cells. These pairs were compared with the most intensely stained areas in each. Scale bar, 50 μm. *P < .05

TABLE 2 Association between *GET4* mRNA expression of tumor tissues and clinicopathologic factors in colorectal cancer

Factors	High expression (n = 61)	Low expression (n = 61)	P value
Age (y)			
<65	22	21	.85
≥65	39	40	
Gender			
Male	32	34	.72
Female	29	27	
Histology			
Well/moderately	57	57	1.00
Poorly	4	4	
Depth of invasion			
M/SM/MP	14	15	.83
SS/SE/SI	47	46	
Lymphatic invasion			
Absent	32	36	.47
Present	29	25	
Lymph node metastasis			
Absent	26	32	.28
Present	35	29	
Venous invasion			
Absent	32	46	<.05
Present	29	15	
Distant metastasis			
Absent	58	61	.08
Present	3	0	
UICC TNM stage			
I, II	25	30	.36
III, IV	36	31	

Abbreviations: M, mucosa; MP, muscular propria; SE, serosal invasion; SI, invasion to adjacent organs; SM, submucosa; SS, subserosa.

significantly associated with a lower OS rate (Table 1). The multivariate analysis showed that poor histology, lymphatic invasion, lymph node metastasis, and high *GET4* mRNA expression were independent poor prognostic factors in CRC (Table 1). These results showed that high *GET4* mRNA expression indicates a poor prognosis in patients with CRC.

3.3 | Clinicopathologic significance of *GET4* mRNA expression in CRC tumor tissues

We analyzed the association between *GET4* mRNA expression and clinicopathologic factors in CRC patients at our hospital (Table 2). We found that the high *GET4* mRNA expression group (n = 61) showed a higher frequency of venous invasion than the low expression group (n = 61). However, there were no significant associations between *GET4* mRNA expression and age, gender, poor histology, depth of invasion, lymphatic invasion, lymph node metastasis, distant metastasis, or clinical stage. These results showed *GET4* mRNA expression is positively associated with the malignant phenotype through venous invasion.

3.4 | BAG6 mainly localizes to the cytoplasm in CRC cells

The *BAG6* mRNA expression in tumor tissues was no different from that in normal tissues (Figure 1F).[9] However, the nuclear/cytoplasmic ratio of BAG6 intensity in tumor cells was lower than in normal colon epithelial cells (Figure 1G). Survival analysis showed that the *BAG6* mRNA expression level did not affect OS in the dataset from TCGA (Figure 1H). In addition, there are only 3.7% of *BAG6* gene alterations with mutations in CRC of the COSMIC dataset (Figure 1I).

These results indicate that the localization of BAG6 has a more important role in CRC progression than its expression level. This finding supports our hypothesis that GET4 could be a critical factor in CRC by regulating the localization of BAG6.

## 3.5 | *UBL4A* mRNA expression in CRC

Ubiquitin-like protein 4A (*UBL4A*), another component of the BAG6 complex, was expressed at higher levels in CRC tissues than in normal tissues (Figure S1B).[4] However, the *UBL4A* mRNA expression levels did not affect OS as determined in TCGA dataset (Figure S1C). These results suggest that GET4, rather than UBL4A, has a major role in CRC progression.

3.6 | *GET4* is overexpressed in various cancers

We assessed the mRNA expression of *GET4* in various cancers, including CRC, in 15 types of tumor tissues and corresponding
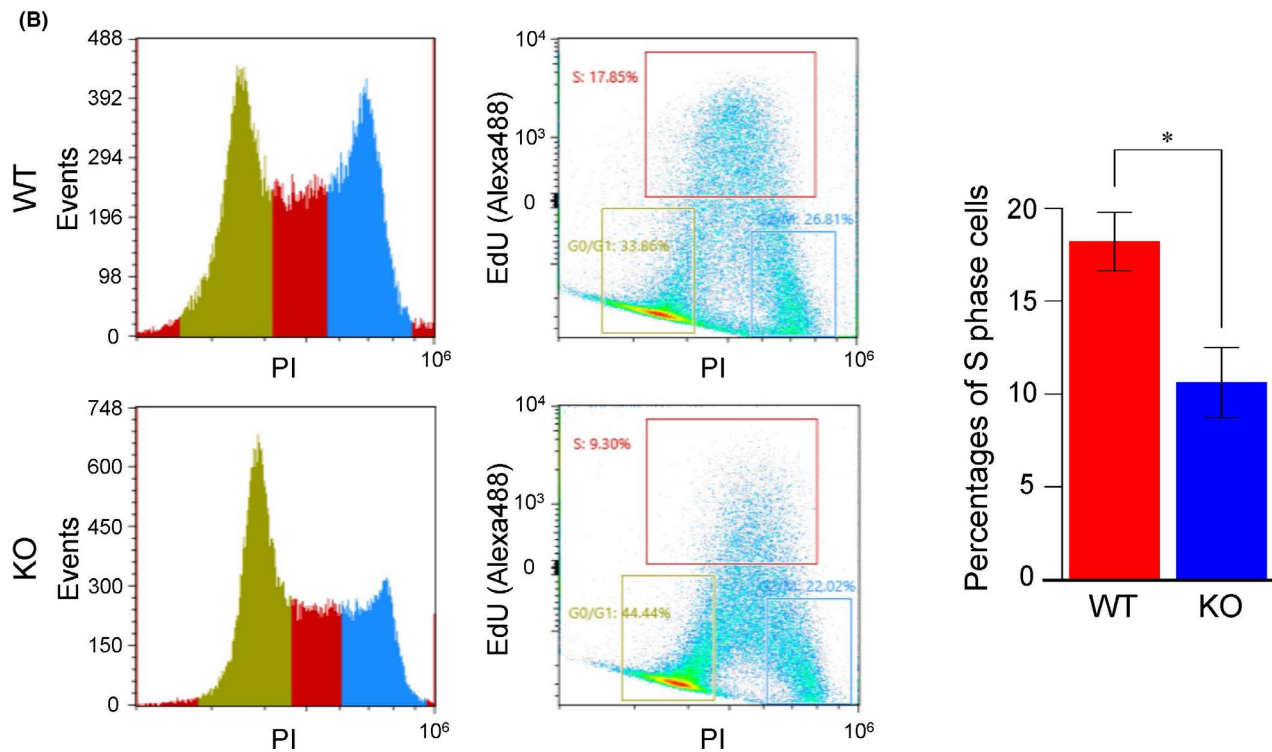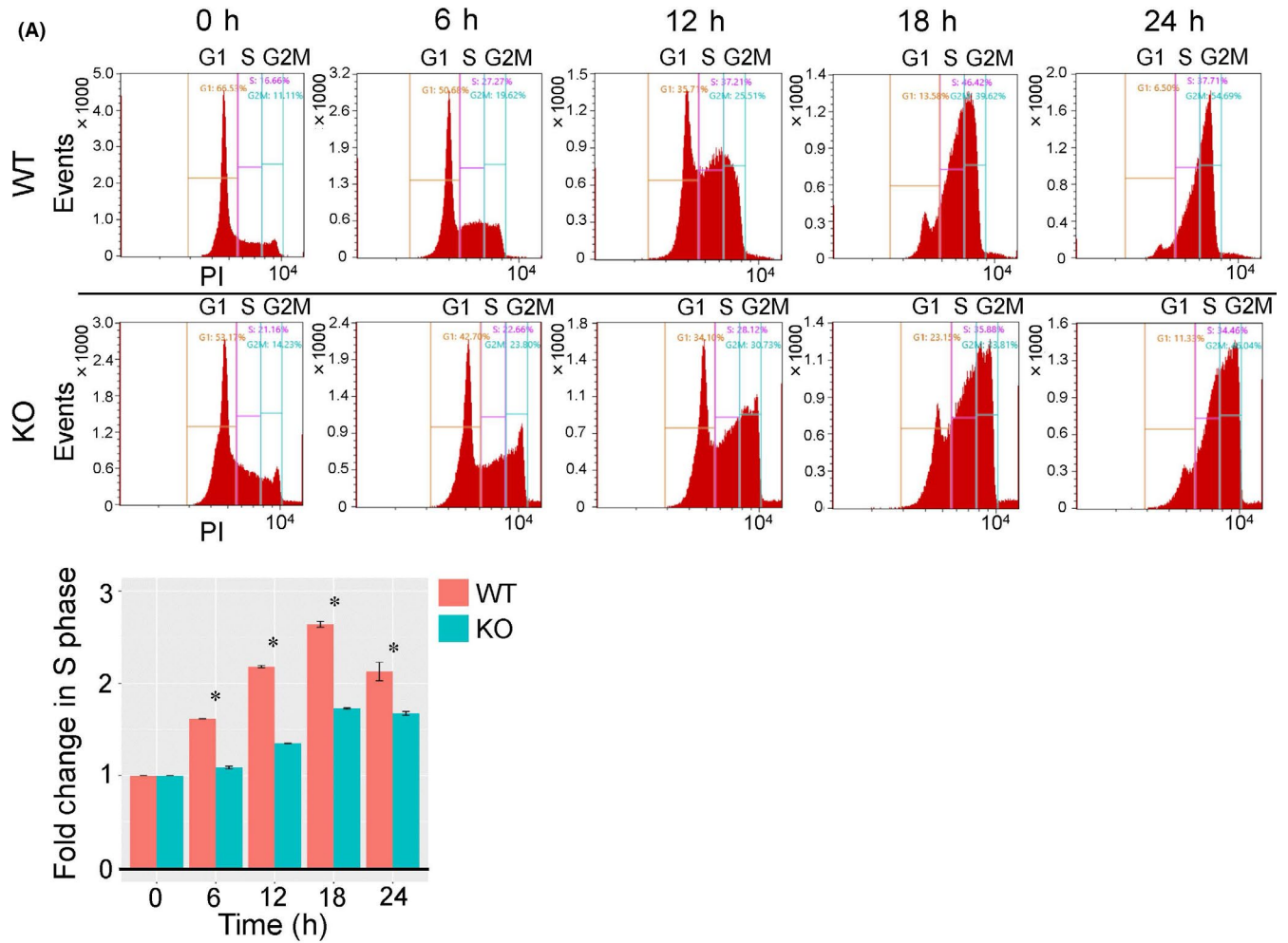
FIGURE 3 Effects of GET4 KO on the cell cycle in colorectal cancer (CRC) cells. Knockout of GET4 suspended cell cycle progression of CRC cells. A, Cell cycle assay of WT cells and GET4 KO cells after serum starvation for 96 h. Propidium iodide (PI) staining was carried out after refeeding of FBS for the indicated time periods. Bar graphs represent the fold change in the proportion of S-phase distribution. B, Representative flow cytometry plots of EdU incorporation in GET4 KO cells and WT cells. Bar graphs represent the proportion of S-phase distribution. *$P < .05$

noncancerous tissues using TCGA datasets (Figure S1D). Interestingly, *GET4* mRNA expression was significantly higher in tumor tissues than noncancerous tissues in all malignancies except CHOL, PAAD, ESCA, and GBM (Figure S1D).

In addition, we evaluated the GET4 protein expression in various cancer cell lines including CRC (colo205, colo320, SW480, and SW620), gastric cancer (MKN45), esophageal squamous cell carcinoma (TE6), lung adenocarcinoma (H1650), hepatocellular carcinoma (HepG2 and PLC), and cholangiocarcinoma (RBE) by immunoblotting. GET4 was expressed in various types of cancer cell lines (Figure S2A,B).

These results provide evidence that GET4 plays an oncogenic role in various cancers.

3.7 | Knockout of GET4 inhibits proliferation of CRC cells in vitro

It has been reported that GET4 regulates the localization of BAG6.[9] In addition, BAG6 appears to promote CRC tumor growth.[9,14] We hypothesized that GET4 could promote tumor growth by facilitating cell cycle progression. First, we observed that endogenous *GET4* mRNA expression was higher in SW620 and SW480 cells than the others based on RT-qPCR results from several CRC cell lines (Figure S2A). Thus, SW620 and SW480 cells were used for subsequent knockdown or KO experiments. To investigate the role of GET4 on CRC growth, we knocked out GET4 in CRC cell lines using the CRISPR/Cas9 system. Genotyping by direct sequencing, RT-PCR, and immunoblotting were undertaken to confirm its KO (Figure 2A). We then showed that GET4 KO significantly reduced colony formation (Figure 2B). Similarly, GET4 knockdown using siRNA also showed decreased proliferative ability (Figure S2C,D).

Furthermore, GET4 KO cells were transiently transfected with a vector expressing GET4 to rescue GET4 expression. Western blot analysis confirmed that GET4 expression was rescued in GET4 KO SW620 and SW480 cells (Figure 2C). Rescue of GET4 expression in GET4 KO cells restored the proliferative capacity of these cells (Figure 2C).

Taken together, these results suggest that GET4 promotes cell proliferation of CRC in vitro.

3.8 | Knockout of GET4 inhibits tumor growth in CRC in vivo

Knockout of GET4 decreased CRC tumor volumes in xenograft mice models (Figure 2D). Immunohistochemical analysis of tumor xenografts revealed that tumor tissues from GET4 KO SW620 cells

displayed weaker GET4 and Ki-67 staining than WT cells (Figure 2E). These results indicate that GET4 could promote tumor growth in vivo in CRC.

3.9 | Knockout of GET4 suppresses cell cycle progression in CRC cells

We undertook cell cycle analysis using flow cytometry. We observed that GET4 KO decreased the S phase fraction (Figure 3A). The EdU assay also showed that the percentage of EdU-positive cells (cells in S phase) in GET4 KO cells was significantly lower than in WT cells in the medium containing 10% FBS (Figure 3B). These data suggest that GET4 should facilitate CRC cell proliferation by promoting the G_1/S transition of the cell cycle. [Correction added on 18 December 2021, after first online publication: In section 3.9 of Results, the word 'higher' in the second sentence was corrected to 'lower' in this version.]

3.10 | Knockout of GET4 inhibits the accumulation of BAG6 in the cytosol, resulting in p53 acetylation and subsequent p21 upregulation

Nuclear localization of BAG6 is necessary for DNA damage-induced acetylation of p53.[12] Acetylation of p53 has important roles in activating tumor suppressor proteins in CRC.[30,31] We examined the effect of GET4 on BAG6 localization using GET4 KO cells. Immunofluorescent analyses of GET4 KO cells showed an apparent accumulation of BAG6 in the nucleus (Figure 4A). To further test whether nuclear BAG6 is necessary for p53 acetylation, we measured the acetylation of p53 Lys373 levels in GET4 KO cells. Immunoblotting with anti-Ac-p53 (Lys373) Abs showed that the acetylation of p53 Lys373 levels was significantly higher in GET4 KO cells (Figure 4B). p21, a cyclin-dependent kinase inhibitor, represents a major target of p53 activity and regulates cell cycle progression.[32] We observed p21 expression level under DNA damage conditions using doxorubicin in GET4 KO and WT cells.[33] Expectedly, p21 expression level was higher in GET4 KO cells than WT cells, supporting our data that GET4 stimulates cell cycle progression (Figure 5A). In addition, GET4 KO in SW620, whose expression is higher than SW480, had a much stronger effect on the expression levels of its downstream genes compared to SW480 (Figures S2B, 4B, and 5A), providing evidence that the expression level of GET4 affects the malignant phenotype of CRC cells. These data indicate that GET4 induces a cytosolic accumulation of BAG6, resulting in deacetylation of p53 followed by reduced p21 expression in CRC.
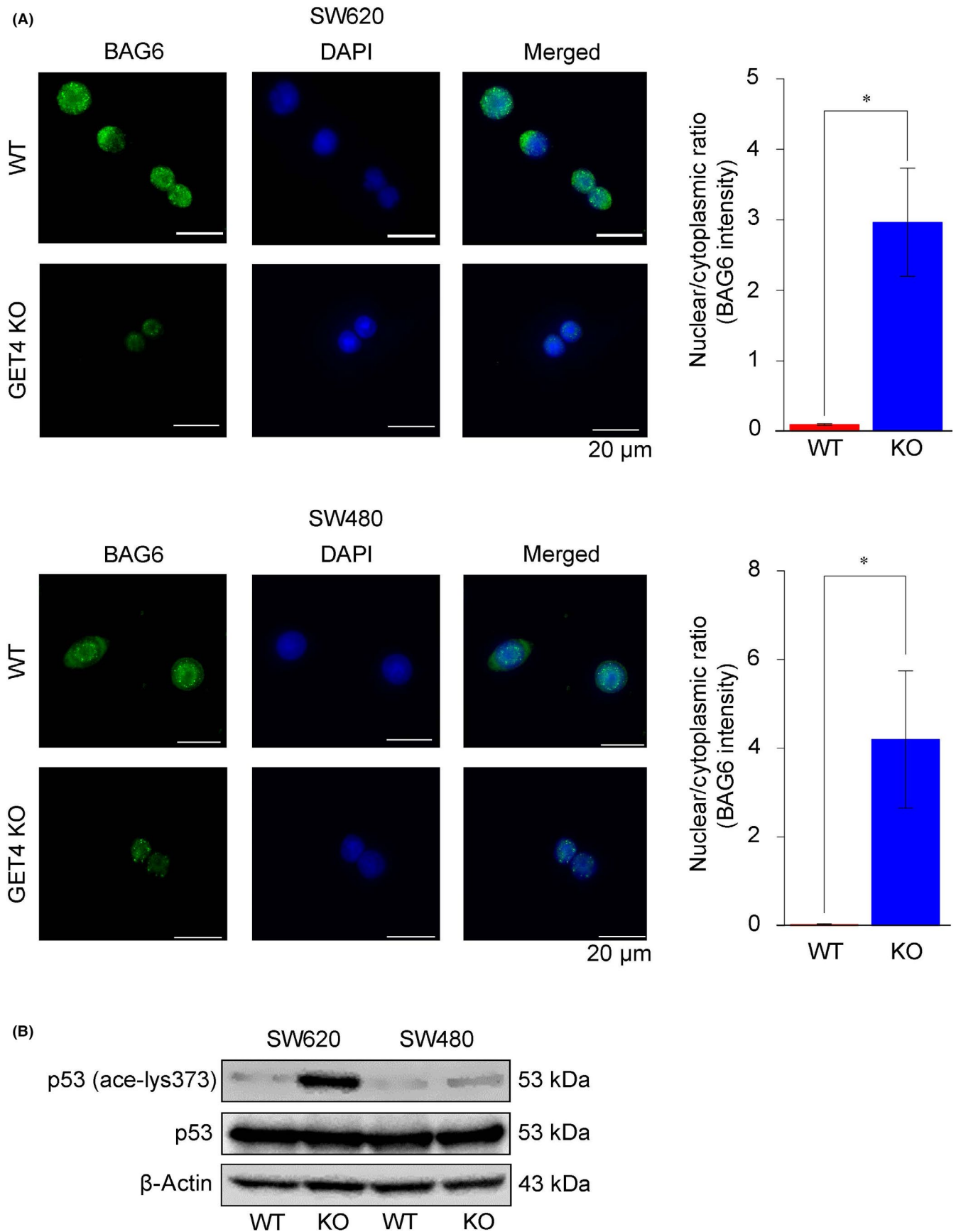
FIGURE 4 GET4 regulates the intracellular localization of BAG6 and the acetylation of p53 in colorectal cancer (CRC) cells. A, Knockout of GET4 increased nuclear localization of BAG6. More than 200 cells were counted in each, and bar graphs show the nuclear / cytoplasmic ratio of BAG6 intensity. *P < .05. B, Immunoblotting for p53 and p53 (ace-lys373) in WT cells and GET4 KO CRC cells

(A)

(B)
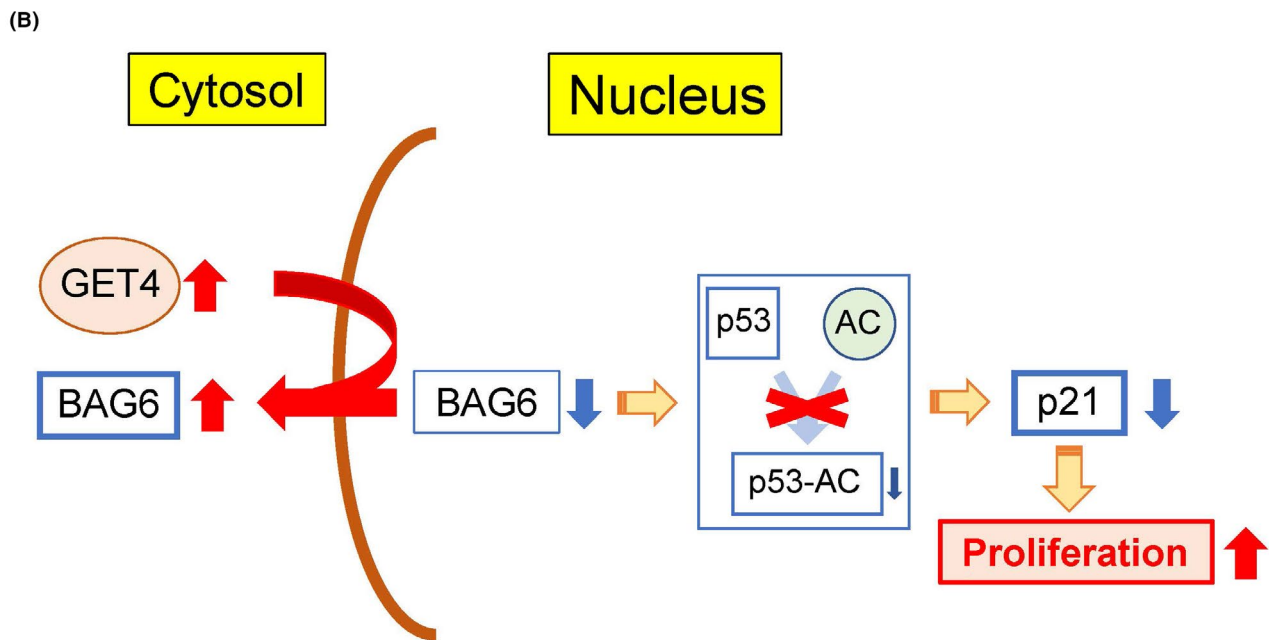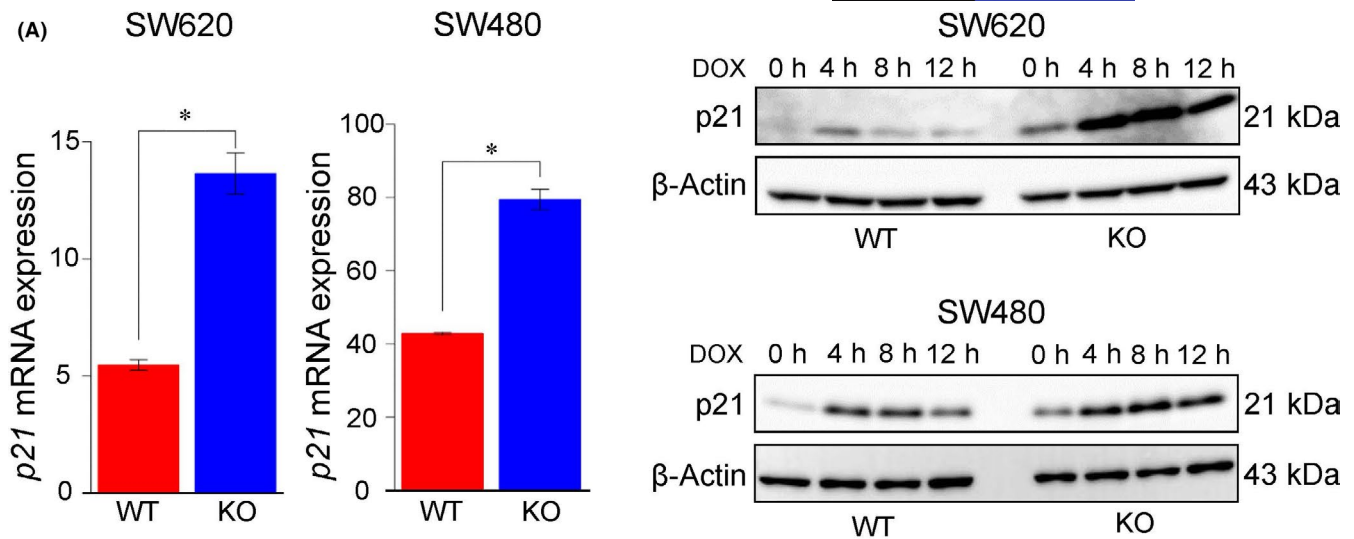
FIGURE 5 Knockout of GET4 upregulates p21 expression in colorectal cancer (CRC) cells. A, Left, RT-quantitative PCR for *p21* mRNA expression normalized to *18s* in WT cells and GET4 KO cells. *P < .05. Right, Immunoblotting for p21 in WT cells and GET4 KO cells that were treated with doxorubicin (DOX, 0.5 μg/mL) and extracted at different time points. B, Schema indicating how GET4 promotes cell cycle progression and tumor proliferation

4 | DISCUSSION

In this study, we found that GET4 contributes to the growth of CRC tumors, possibly by inducing the cytosolic accumulation of BAG6. Furthermore, *GET4* expression predicts the poor prognosis of CRC patients. To our knowledge, this is the first study to show that *GET4* affects not only the malignant phenotypes of CRC but also the clinical outcome of CRC patients.

BCL2-associated athanogene 6 is the central component of a three-protein complex that also includes GET4 and UBL4A.[16,34] GET4, but not UBL4A, can mask the NLS of BAG6, leading to its retention in the cytoplasm.[16] Interestingly, our study showed that *UBL4A* mRNA expression did not affect OS, but *GET4* mRNA expression did influence OS. These findings indicated that GET4, rather than UBL4A, has a major role in nucleocytoplasmic localization of BAG6 in CRC.[14] Furthermore, we found very few gene alterations of

BAG6 in CRC that might have affected the intracellular location of BAG6. Taken together, we provide evidence that GET4, identified as a potential driver gene on Ch.7p by bioinformatics, primarily regulates the nucleocytoplasmic transport of BAG6 in CRC.

Our clinical study showed that *GET4* mRNA expression was increased due to DNA copy number gain at the *GET4* locus on Ch.7p. The expression of *GET4* was positively associated with the malignant pathological phenotype such as venous invasion, and overexpression of *GET4* was an independent poor prognostic factor in CRC. These findings provide clinical evidence that *GET4* is a potential driver gene, and could be a novel biomarker of poor prognosis in patients with CRC.

Biological analysis showed that GET4 accelerates tumor growth, possibly through facilitating cell cycle progression in CRC. We examined the mechanism by which GET4 promotes cell cycle progression in CRC. Knockout of GET4 reduced the accumulation of BAG6 in the cytosol and promoted the acetylation of p53, which is the critical process for p53 activation.[35-38] Furthermore, using GET4 KO cells, we showed that p53 acetylation induced p21 and inhibited tumor cell growth by suppressing cell cycle progression, data consistent with previous reports.[39-41] These findings indicate that GET4 has a critical role in CRC proliferation by regulating the localization of BAG6, resulting in deacetylation of p53 followed by reduced p21 expression.

Intratumor heterogeneity, which is defined as molecular and cellular heterogeneity within a single tumor, is believed to cause therapeutic difficulties due to the presence of multiple subclones. Here, we showed that *GET4* on Ch.7p is ubiquitously expressed in tumor cells due to their chromosomal amplification in CRC. The overexpression and resulting gain-of-function of GET4 could be a spatiotemporal driver event shared in the evolution of CRC. Therefore, GET4 could be a promising target to overcome therapeutic resistance conferred by tumor heterogeneity.

In summary, our study showed that *GET4* is a novel CRC driver gene on Ch.7p. It promoted tumor growth by facilitating cell cycle progression, possibly through increased cytosolic localization of BAG6, which is an essential key regulator of p53 acetylation. GET4 could be a therapeutic target as well as a prognostic biomarker in CRC.

DISCLOSURE

No potential conflicts of interest were disclosed.

ORCID

Kensuke Koike https://orcid.org/0000-0003-4428-2348
Kuniaki Sato https://orcid.org/0000-0001-6014-1911
Koshi Mimori https://orcid.org/0000-0003-3897-9974

REFERENCES

1. Keum N, Giovannucci E. Global burden of colorectal cancer: emerging trends, risk factors and prevention strategies. *Nat Rev Gastroenterol Hepatol*. 2019;16:713-732.
2. Jemal A, Bray F, Center MM, Ferlay J, Ward E, Forman D. Global cancer statistics. *CA Cancer J Clin*. 2011;61:69-90.
3. Katona BW, Weiss JM. Chemoprevention of Colorectal Cancer. *Gastroenterology*. 2020;158:368-388.
4. Binici J, Koch J. BAG-6, a jack of all trades in health and disease. *Cell Mol Life Sci*. 2014;71:1829-1837.
5. Hessa T, Sharma A, Mariappan M, Eshleman HD, Gutierrez E, Hegde RS. Protein targeting and degradation are coupled for elimination of mislocalized proteins. *Nature*. 2011;475:394-397.
6. Kawahara H, Minami R, Yokota N. BAG6/BAT3: emerging roles in quality control for nascent polypeptides. *J Biochem*. 2013;153:147-160.
7. Lee JG, Ye Y. Bag6/Bat3/Scythe: a novel chaperone activity with diverse regulatory functions in protein biogenesis and degradation. *BioEssays*. 2013;35:377-385.
8. Payapilly A, High S. BAG6 regulates the quality control of a polytopic ERAD substrate. *J Cell Sci*. 2014;127:2898-2909.
9. Mock JY, Xu Y, Ye Y, Clemons WM Jr. Structural basis for regulation of the nucleo-cytoplasmic distribution of Bag6 by TRC35. *Proc Natl Acad Sci U S A*. 2017;114:11679-11684.
10. Krenciute G, Liu S, Yucer N, et al. Nuclear BAG6-UBL4A-GET4 complex mediates DNA damage signaling and cell death. *J Biol Chem*. 2013;288:20547-20557.
11. Yong ST, Wang XF. A novel, non-apoptotic role for Scythe/BAT3: a functional switch between the pro- and anti-proliferative roles of p21 during the cell cycle. *PLoS One*. 2012;7:e38085.
12. Sasaki T, Gan EC, Wakeham A, Kornbluth S, Mak TW, Okada H. HLA-B-associated transcript 3 (Bat3)/Scythe is essential for p300-mediated acetylation of p53. *Genes Dev*. 2007;21:848-861.
13. Sebti S, Prébois C, Pérez-Gracia E, et al. BAT3 modulates p300-dependent acetylation of p53 and autophagy-related protein 7 (ATG7) during autophagy. *Proc Natl Acad Sci U S A*. 2014;111:4115-4120.
14. Wu W, Song W, Li S, et al. Regulation of apoptosis by Bat3-enhanced YWK-II/APLP2 protein stability. *J Cell Sci*. 2012;125:4219-4229.
15. Manchen ST, Hubberstey AV. Human Scythe contains a functional nuclear localization sequence and remains in the nucleus during staurosporine-induced apoptosis. *Biochem Biophys Res Commun*. 2001;287:1075-1082.
16. Wang Q, Liu Y, Soetandyo N, Baek K, Hegde R, Ye Y. A ubiquitin ligase-associated chaperone holdase maintains polypeptides in soluble states for proteasome degradation. *Mol Cell*. 2011;42:758-770.
17. Davoli T, Xu AW, Mengwasser KE, et al. Cumulative haploinsufficiency and triplosensitivity drive aneuploidy patterns and shape the cancer genome. *Cell*. 2013;155:948-962.
18. Uchi R, Takahashi Y, Niida A, et al. Integrated multiregional analysis proposing a new model of colorectal cancer evolution. *PLoS Genet*. 2016;12:e1005778.
19. Saito T, Niida A, Uchi R, et al. A temporal shift of the evolutionary principle shaping intratumor heterogeneity in colorectal cancer. *Nat Commun*. 2018;9:2884.
20. Calabrese C, Davidson NR, Demircioğlu D, et al. Genomic basis for RNA alterations in cancer. *Nature*. 2020;578:129-136.

21. Sato K, Masuda T, Hu Q, et al. Novel oncogene 5MP1 reprograms c-Myc translation initiation to drive malignant phenotypes in colorectal cancer. *EBioMedicine*. 2019;44:387-402.

22. Shimizu D, Masuda T, Sato K, et al. CRMP5-associated GTPase (CRAG) is a candidate driver gene for colorectal cancer carcinogenesis. *Anticancer Res*. 2019;39:99-106.

23. Sato K, Masuda T, Hu Q, et al. Phosphoserine phosphatase is a novel prognostic biomarker on chromosome 7 in colorectal cancer. *Anticancer Res*. 2017;37:2365-2371.

24. Kouyama Y, Masuda T, Fujii A, et al. Oncogenic splicing abnormalities induced by DEAD-Box Helicase 56 amplification in colorectal cancer. *Cancer Sci*. 2019;110:3132-3144.

25. Garmire LX, Subramaniam S. Evaluation of normalization methods in mammalian microRNA-Seq data. *RNA (New York, NY)*. 2012;18:1279-1288.

26. Masuda TA, Inoue H, Nishida K, et al. Cyclin-dependent kinase 1 gene expression is associated with poor prognosis in gastric carcinoma. *Clinical Cancer Res*. 2003;9:5693-5698.

27. Nambara S, Iguchi T, Oki E, Tan P, Maehara Y, Mimori K. Overexpression of CXCR7 Is a novel prognostic indicator in gastric cancer. *Dig Surg*. 2017;34:312-318.

28. Hirata H, Sugimachi K, Komatsu H, et al. Decreased expression of fructose-1,6-bisphosphatase Associates with Glucose Metabolism and Tumor Progression in Hepatocellular Carcinoma. *Cancer Res*. 2016;76:3265-3276.

29. Fujii A, Masuda T, Iwata M, et al. The novel driver gene ASAP2 is a potential druggable target in pancreatic cancer. *Cancer Sci*. 2021;112:1655-1668.

30. Marouco D, Garabadgiu AV, Melino G, Barlev NA. Lysine-specific modifications of p53: a matter of life and death? *Oncotarget*. 2013;4:1556-1571.

31. Wang J, Qian J, Hu Y, et al. ArhGAP30 promotes p53 acetylation and function in colorectal cancer. *Nat Commun*. 2014;5:4735.

32. Harper JW, Adami GR, Wei N, Keyomarsi K, Elledge SJ. The p21 Cdk-interacting protein Cip1 is a potent inhibitor of G1 cyclin-dependent kinases. *Cell*. 1993;75:805-816.

33. Momparler RL, Karon M, Siegel SE, Avila F. Effect of adriamycin on DNA, RNA, and protein synthesis in cell-free systems and intact cells. *Cancer Res*. 1976;36:2891-2895.

34. Mariappan M, Li X, Stefanovic S, et al. A ribosome-associating factor chaperones tail-anchored membrane proteins. *Nature*. 2010;466:1120-1124.

35. Levine AJ, Oren M. The first 30 years of p53: growing ever more complex. *Nat Rev Cancer*. 2009;9:749-758.

36. Bode AM, Dong Z. Post-translational modification of p53 in tumorigenesis. *Nat Rev Cancer*. 2004;4:793-805.

37. Brooks CL, Gu W. The impact of acetylation and deacetylation on the p53 pathway. *Protein Cell*. 2011;2:456-462.

38. Li Q, Hao Q, Cao W, et al. PP2Cδ inhibits p300-mediated p53 acetylation via ATM/BRCA1 pathway to impede DNA damage response in breast cancer. *Sci Adv*. 2019;5:eaaw8417.

39. Liu Y, Tavana O, Gu W. p53 modifications: exquisite decorations of the powerful guardian. *J Mol Cell Biol*. 2019;11:564-577.

40. Reed SM, Quelle DE. p53 Acetylation: regulation and consequences. *Cancers (Basel)*. 2014;7:30-69.

41. Zhao Y, Lu S, Wu L, et al. Acetylation of p53 at lysine 373/382 by the histone deacetylase inhibitor depsipeptide induces expression of p21(Waf1/Cip1). *Mol Cell Biol*. 2006;26:2782-2790.

SUPPORTING INFORMATION

Additional supporting information may be found in the online version of the article at the publisher's website.